Fibroblast growth factor 23 inhibits osteogenic differentiation and mineralization of chicken bone marrow mesenchymal stem cells

Zhengtian Lyu,[†,1] Haifang Li,[*,1] Xin Li,[†] Hui Wang,[†] Hongchao Jiao,[†] Xiaojuan Wang,[†] Jingpeng Zhao,[†] and Hai Lin[†,2]

[*]*Department of Life Science, Shandong Agricultural University, Taian City, Shandong Province, 271018, China; and* [†]*Department of Animal Science, Shandong Agricultural University, Key Laboratory of Efficient Utilization of Non-grain Feed Resources (Co-construction by Ministry and Province), Ministry of Agriculture and Rural Affairs, Shandong Key Lab for Animal Biotechnology and Disease Control and Prevention, Taian City, Shandong Province, 271018, China*

ABSTRACT Fibroblast growth factor 23 (**FGF23**), a bone-derived hormone, is involved in the reabsorption of phosphate (**P**) and the production of vitamin D hormones in the kidney. However, whether and how FGF23 regulates chicken bone metabolism remains largely unknown. In the present study, we investigated the effect of FGF23 on osteogenic differentiation and mineralization of chicken bone marrow mesenchymal stem cells (**BMSCs**). First, we found that the transcription of FGF23 was inhibited by β-glycerophosphate sodium (**GPS**, 5 mM, 10 mM, 20 mM) and 10^{-9} M 1, 25-dihydroxyvitamin D3 (**1, 25(OH)$_2$D$_3$**), but was stimulated by 10^{-7} M 1, 25(OH)$_2$D$_3$ and parathyroid hormone (**PTH**, 10^{-9} M, 10^{-8} M, 10^{-7} M). Second, overexpression of FGF23 by the FGF23 adenovirus (**Adv-FGF23**) suppressed the formation of mineralized nodules ($P < 0.001$) and alkaline phosphatase (**ALP**) activity ($P < 0.05$) in both differentiated and mineralized osteoblasts. Administration of FGF receptor 3 (**FGFR3**) inhibitor (50 nM) was sufficient to restore the FGF23-decreased ALP activity ($P < 0.05$), but not for the formation of mineralized nodules. In addition, the phosphorylation of ERK increased considerably with Adv-FGF23 overexpression ($P < 0.05$). Administration of an ERK-specific inhibitor (10 μM) could down-regulate the phosphorylation of ERK (**P-ERK**) ($P < 0.05$) and slightly restored the Adv-FGF23-reduction of ALP activity ($P = 0.08$). In summary, our data suggest that GPS, 1, 25(OH)$_2$D$_3$, and PTH could regulate *FGF23* mRNA expression in vitro. FGF23 is a negative regulator of bone remodeling. FGF23 not only inhibits BMSCs osteogenesis through the FGFR3-ERK signaling pathway but also suppresses the mineralization of mature osteoblasts.

Key words: BMSC, FGF23, osteogenesis, mineralization, the ERK signaling

2023 Poultry Science 102:102287
https://doi.org/10.1016/j.psj.2022.102287

INTRODUCTION

Since its discovery, fibroblast growth factor 23 (**FGF23**) has been considered a key regulator of phosphate (**P**) and vitamin D3 (**VD$_3$**) metabolism (Consortium, 2000; Shimada et al., 2004; Erben, 2018). FGF23, which is synthesized and secreted by osteocytes and late differentiated osteoblasts, involves P regulation by inhibiting P reabsorption in the kidney (Yoshiko et al., 2007; Fernandes-Freitas and Owen, 2015). Unlike the other classical fibroblast growth factors (**FGFs**), which activate the cell surface canonical FGF receptors (**FGFR**) by binding with the heparin sulfate matrix, the hormone-like FGFs (FGF19, FGF21, and FGF23) lack heparin-binding domains. The lack of heparin affinity makes FGF23 dependent on an alternative cofactor, Klotho, to elicit a signal on target cells (Li et al., 2013) and to play a role in regulating P reabsorption and excretion (Kurosu et al., 2006; Urakawa et al., 2006). In addition, FGF23 is also associated with bone metabolism. Excess FGF23 could lead to defects in skeletal growth and development, as in patients with X-linked hypophosphatemic rickets. Patients with tumor-induced osteomalacia also exhibit high FGF23 levels, phosphate wasting, and skeletal abnormalities (Simic and Babitt, 2021). High serum FGF23 level was suggested as a biomarker in predicting osteoporosis (Shen et al., 2017).

Received May 24, 2022.
Accepted October 20, 2022.

[1]These authors contributed equally to this work.

[2]Corresponding author. hailin@sdau.edu.cn

In laying hens, P is essential in the maintenance of productive performance and eggshell quality (Schreiweis et al., 2003; Li et al., 2018). P is maintained at a narrow equilibrium range by a complex hormone regulation network mainly consisting of parathyroid hormone (**PTH**) and 1, 25-dihydroxyvitamin D3 (**1, 25 $(OH)_2D_3$**). The homeostasis of P is balanced by the absorption in the small intestine, reabsorption, and excretion by the kidney, deposition, and mobilization of bone (Li et al., 2018). P is also crucial in the extracellular matrix mineralization of osteoblasts (Ahmad and Balander, 2003). However, the regulating effect of FGF23 on calcium and phosphorus metabolism is known little in laying hens. Injection of the FGF23 antibody in layers significantly reduces the level of FGF23 and P excretion. This corresponds to the serum P being increased (Ren et al., 2017). In our previous research, a high-phosphorus diet significantly upregulated *FGF23* mRNA expression in the skull, femur, and tibia (Wang et al., 2018). These findings of FGF23 associated with P homeostasis in chickens suggest the potential of FGF23 on the mineralization of osteoblasts, which could assist in understanding the regulation network of P in laying hens.

The chicken bone is an attractive research model due to its higher rate of mineralization and unique bone turnover process (Whitehead, 2004; Pande et al., 2015). Medullary bone is a non-structural woven bone unique to egg-laying birds in the marrow cavity, and functions as a calcium supplier for eggshell formation (Fleming et al., 1998). During the daily egg-laying cycle, medullary bone constantly undergoes remodeling, which is a balance between osteoblast-mediated bone formation and osteoclast-mediated bone resorption (Tan et al., 2015). During bone remodeling, osteoclasts release calcium from the bone and digest the collagenous bone matrix, after which osteoblasts form and mineralize the collagen matrix (Kerschnitzki et al., 2014). Osteoblasts are bone-forming cells originating from the bone marrow mesenchymal stem cells (**BMSCs**) (Okamoto et al., 2017). BMSCs are multipotent stromal cells that can differentiate into a variety of cell types, including osteoblasts, chondrocytes, myocytes, and adipocytes (Fierabracci et al., 2015). BMSCs have been isolated from many species, including chickens, sheep, cats, dogs, rats, mice, and humans (Svoradova et al., 2021). The directional differentiation of BMSCs was determined by the presence of different stimuli (Niu et al., 2021). BMSC can be used as an avian culture model to better understand osteogenic process due to their easy isolation, and in vitro proliferation (Eleuteri and Fierabracci, 2019).

Recently, it is proved that FGF23 is expressed in medullary bone and synchrony with the egg-laying cycle (Hadley et al., 2016). Hence, we hypothesized that FGF23 regulates the mineralization of chicken osteoblasts. In this study, the effect of P, VD_3, and PTH on the expression of FGF23 in osteoblasts was investigated in vitro. Thereafter, the effect of FGF23 overexpression on mineralization of BMSCs-derived osteoblasts was determined at both differentiation and mineralization stages. Furthermore, the involvement of FGFR3 and the ERK signaling in the FGF23 action was investigated.

MATERIALS AND METHODS

Isolation and Culture of Chicken BMSCs

All procedures in the study were approved by the Animal Care Committee of Shandong Agricultural University and were performed following the guidelines for experimental animals of the Ministry of Science and Technology (Beijing, China).

Specific pathogen-free chicken eggs were obtained (Jinan SAIS Poultry Co., LTD.) and hatched in an incubator (Haijiang, Beijing, China). At the embryo age of 18 d, the femur and tibia of the chicken embryos were separated. After removing the attached muscles, the medullary cavity was rinsed with a 1 mL syringe to collect the **BMSC**s. The BMSCs isolated from every 2 embryos could satisfy a 6-well cell culture plate. A total of 80 embryos were used in this study.

BMSCs were cultured in low-glucose Dulbecco's modified Eagle's medium (DMEM; HyClone, Thermo Fisher, Shanghai, China) supplemented with 10% FBS (Gibco, Grand Island, New York) and 1% penicillin/streptomycin (Solarbio, Beijing, China). To ensure the mineralization of BMSCs, 50 μg/mL L-ascorbic acid (Aladdin, China), 10 mM β-glycerophosphate disodium salt (**GPS**, Aladdin, China), and 0.01 μM dexamethasone (Solarbio, Beijing, China) was added to the culture medium as the osteogenic medium. Cells were cultured in a humidified 5% CO_2 atmosphere at 37°C.

Construction and Identification of FGF23 Adenovirus

According to the sequence alignment (Gallus FGF23, XP_425663.1), there is also an RXXR proteolytic cleavage site in the FGF23 amino acid sequence of laying hens. Mutation of RXXR prevents the degradation of FGF23 (Alizadeh Naderi and Reilly, 2010). When synthesizing the FGF23 plasmid, the AGA, which is encoded arginine, was sited-specifically mutated to the CAA, which is encoded glutamine. The construction of the plasmid was completed by Sangon (Shanghai, China). The FGF23 plasmid was packaged as FGF23 adenovirus (**Adv-FGF23**) by Vigene (Jinan, China). The total titer of the Adv-FGF23 was 1.2×10^{11} pfu/mL. To determine whether the transfection was successful, an inverted fluorescence microscope was used to observe the green fluorescent protein (**GFP**) signal.

Cell Treatment

To determine the effect of P, VD_3, and PTH on the expression of FGF23, mineralized osteoblasts were treated with 5 mM, 10 mM, and 20 mM GPS (D106347,

Aladdin, China), 10^{-9} M, 10^{-8} M, and 10^{-7} M 1, 25 $(OH)_2D_3$ (C120126, Aladdin, China), 10^{-9} M, 10^{-8} M, and 10^{-7} M PTH (SCP0231, Sigma) at day 12 for 48 h, respectively.

To determine whether FGF23 adenovirus can be stably infected osteoblasts, the mineralized osteoblasts were treated with 10^7 pfu/mL empty vector adenovirus with GFP tagging (**Adv-GFP**), 10^6 pfu/mL Adv-FGF23, and 10^7 pfu/mL Adv-FGF23 at day 12 for 48 h.

Differentiated osteoblasts were treated with 10^7 pfu/mL Adv-GFP, 10^7 pfu/mL Adv-FGF23 alone, or in combination with 50 nM FGF receptor 3 (**FGFR3**) inhibitor (FGF/VEGF receptor tyrosine kinase inhibitor, 341607, Sigma) or 10 μM MAPK kinase inhibitor (PD98059, Beyotime, China) respectively at day 4 for 10 d.

In the mineralization stage, cells were treated with 10^7 pfu/mL Adv-GFP, 10^7 pfu/mL Adv-FGF23 alone, or in combination with 50 nM FGFR3 inhibitor or 10 μM ERK-specific inhibitor respectively at day 12 for 48 h.

Determination of Alkaline Phosphatase (ALP) Activity

For ALP in vitro chemical assays, osteoblasts were suspended in 0.3 mL normal saline after treatment according to the ALP kit instructions (Nanjing Jiancheng, China). An aliquot of cell lysate was mixed with the ALP substrate buffer, and the mixture was incubated at 37°C for 15 min. After adding 150 μL of a chromogenic agent, the OD (optical density) values were measured at 520 nm. The amount of ALP required to decompose the substrate to produce 1 mg of phenol at 37℃ for 15 min was defined as 1U. The ALP activity was normalized to total protein determined using a BCA assay kit (Beyotime, China), which was expressed as U/g protein.

Measurement of Mineralized Nodules in BMSCs via Alizarin red S (ARS) Staining

For ARS staining, the cells were fixed with 95% ethanol for 30 min after being washed with PBS. Following further rinsing with PBS, cells were stained with ARS (40 mM, pH 4.2, Solarbio, China) for 30 min at room temperature. Unincorporated dye was washed with PBS, then the final wash was aspirated and the plate was left to dry for imaging. Finally, the content of each well was solubilized with 10% (w/v) cetylpyridinium chloride (Bio basic, Markham ON, Canada) for 15 min. The absorbance was read in duplicate at 570 nm with a 96-well plate reader.

RNA Extraction and Quantitative Real-time PCR (qPCR) Analysis

Total RNA was extracted with the TRIzol Reagent (Invitrogen, San Diego, CA) according to the RNA isolation procedure from nonbone tissues. RNA quality was determined with agarose gel electrophoresis and a photometer (Eppendorf, Germany) detecting the UV absorbance ratio at 260 nm and 280 nm. The cDNA was synthesized using a reverse transcription-polymerase chain reaction kit (Roche, Germany). The reaction was performed in a volume of 20 μL containing 1,000 ng total RNA, 60 μM/L random hexamer primer, 8 mmol/L $MgCl_2$, 20 U RNase inhibitor, 1 mmol/L dNTP, 10 U reverse transcriptase and PCR-grade water.

Real-time qPCR was carried out on ABI 7500 PCR machine (Applied Biosystems; Thermo, MA, USA) using the FastStart Universal SYBR Green Master (Rox) (Roche, Switzerland). Primer sequences are shown in Table 1. Average Ct values from triplicates were normalized from average Ct values of β-actin. The relative expression levels of mRNA were calculated by the $2^{-\Delta\Delta Ct}$ method.

Protein Preparation and Western Blot Analysis

Osteoblasts were homogenized in 0.2 mL of lysis buffer (Beyotime, China) and kept on ice during the trial procedure. The homogenate was centrifuged at 12,000 g for 5 min at 4°C, and the supernatant was collected. Protein concentration was assayed using a BCA assay kit (Beyotime, China) according to the manufacturer's protocol. Aliquots of 18 μg of protein were separated with 7.5 to 10% SDS polyacrylamide gels (Bio-Rad, Richmond, 246 CA), and the proteins were then transferred onto a PVDF membrane (Millipore, Darmstadt, Germany) at 200 mA for 2 h in a Tris-glycine buffer with 20% anhydrous ethanol at 4° C. Membranes were blocked with the western blocking buffer (Beyotime, China) for 1 h at room temperature. The membranes were then probed with primary antibodies at 4°C with gentle shaking overnight. The primary antibodies used were anti-FGF23 (ABClonal, China), anti-ERK (CST), anti-phospho-ERK (CST, MA, USA), and anti-α-Tubulin (Beyotime, China). After being washed, the membranes were incubated with horseradish peroxidase-linked anti-rabbit secondary antibodies for 4 h at 4°C. Membranes were then visualized by exposure to Hyperfilm ECL (Beyotime, China). Films were scanned, and

Table 1. Gene-specific primer of related genes.

Gene	Primer sequences 5'to 3'	Accession NO.
β-actin	Forward-ACCACACCTTCTACAATGAG Reverse-ACGACCAGAGGCATACAG	XM_003357928
FGF23	Forward-AGCTGCCTGGAGTACATGCT Reverse-ATTCAGCAGCGGAGAGGAGT	XM_425663.4
ALP	Forward-GGAGTCTCATTCCTAACGCATCGC Reverse-CCTCTTGGTTGGAGTGCAGCATC	NM_205360.1
FGFR3	Forward-CCAGCAGGTGGAAACCCAACTC Reverse-GATCTGACGGCACAACGCTCTC	NM_205509.3
OPN	Forward-CTGAGGTGGGCGGAGGAGAC Reverse-GCGTCTGGTTGCTGGTGTCG	M_59182.1

ALP, Alkaline phosphorus; FGF23, Fibroblast growth factor 23; FGFR3, Fibroblast growth factor receptor 3; OPN, Osteopontin.

specific bands were quantified using ImageJ 1.43 software (National Institutes of Health, Bethesda, MD, USA). The band intensity was normalized to the α-Tubulin band in the same sample.

Statistical Analysis

The data were analyzed by GraphPad Prism version 8.0 software (GraphPad Software Inc., San Diego, CA) and shown as means ± SD. The main effect of each treatment was evaluated using a one-way ANOVA performed with the Statistical Analysis Systems statistical software package (Version 8e, SAS Institute, NC, USA). The data were considered to be significantly different at $P < 0.05$.

RESULTS

Effect of P, 1, 25(OH)$_2$D$_3$, and PTH on the Expression of FGF23 mRNA in Osteoblasts

To determine the effect of P, VD$_3$, and PTH on mRNA expression of *FGF23*, mineralized osteoblasts were treated with GPS, 1, 25(OH)$_2$D$_3$, and PTH. Treatment with 5 mM, 10 mM, and 20 mM GPS significantly decreased *FGF23* mRNA expression ($P < 0.001$, Figure 1a). *FGF23* mRNA expression was upregulated by PTH ($P < 0.001$, Figure 1b). The effect of 1, 25 (OH)$_2$D$_3$ on *FGF23* mRNA expression was dependent on its concentration. The expression of *FGF23* mRNA was suppressed by 10^{-9} M 1, 25(OH)$_2$D$_3$, whereas upregulated by 10^{-7} M 1, 25(OH)$_2$D$_3$ ($P < 0.001$). However, 10^{-8} M 1, 25(OH)$_2$D$_3$ did not show any effect on *FGF23* mRNA expression ($P > 0.05$, Figure 1c).

Overexpression of FGF23 in Osteoblasts

To prove the effectiveness of the adenovirus, osteoblasts were infected with Adv−GFP and Adv-FGF23. After infection for 48 h, strong fluorescent signals can be detected (Figure 2a), illustrating that adenovirus localized to cells. Consistent with this, qPCR confirmed a marked increase levels of *FGF23* mRNA expression after infection with 10^6 pfu/mL and 10^7 pfu/mL Adv−FGF23 ($P < 0.05$, Figure 2b). Notably, an increased FGF23 protein content was only observed following 10^7 pfu/mL Adv-FGF23 ($P < 0.05$, Figure 2d). Under 10^7 pfu/mL Adv-FGF23, *FGFR3* mRNA levels were increased significantly ($P < 0.05$, Figure 2c). Overexpression of Adv-FGF23 significantly reduced the formation of mineralized nodules, suggesting that FGF23 significantly inhibited the osteogenic effect of BMSCs ($P < 0.05$, Figure 2e). There was no effect of 10^7 pfu/mL Adv-GFP on gene expression and cell mineralization. Thus, 10^7 pfu/mL Adv-GFP and 10^7 pfu/mL Adv-FGF23 were used as the working concentration for subsequent tests.

Effect of Co-Treatment with Adv-FGF23 and FGFR3 Inhibitor on Mineralized Osteoblasts

As a functional receptor of FGF23, *FGFR3* is upregulated by overexpression of FGF23. To investigate whether FGF23 inhibits osteogenesis of BMSCs through FGFR3, mature osteoblasts were treated with Adv-FGF23 alone or in combination with FGFR3 inhibitor.

As shown in Figure 3, *FGF23* mRNA expression was upregulated significantly by the overexpression of Adv-FGF23 despite the presence of FGFR3 inhibitor ($P < 0.001$, Figure 3a). Besides, Adv-FGF23 also led to an increase in osteopontin (***OPN***) mRNA expression ($P < 0.05$, Figure 3b). Conversely, these FGF23-induced enhancements were blocked in the presence of the FGFR3 inhibitor ($P < 0.05$, Figure 3b). A decrease in mineralized nodules was observed in response to overexpression of Adv-FGF23 ($P < 0.05$, Figure 3c, d). However, the administration of FGFR3 inhibitor has no impact on osteoblastic mineralization ($P > 0.05$, Figure 3c, d). To determine the effect of Adv-FGF23 on another bone formation marker, the mRNA expression and enzyme activity of ALP were detected. Adv-FGF23 dramatically down-regulated the *ALP* mRNA expression ($P < 0.05$, Figure 3e). Similarly, *ALP* mRNA expression levels were also decreased after FGFR3 inhibitor treatment regardless of whether Adv-FGF23 was overexpressed ($P < 0.05$, Figure 3e). Further measurements of ALP enzyme

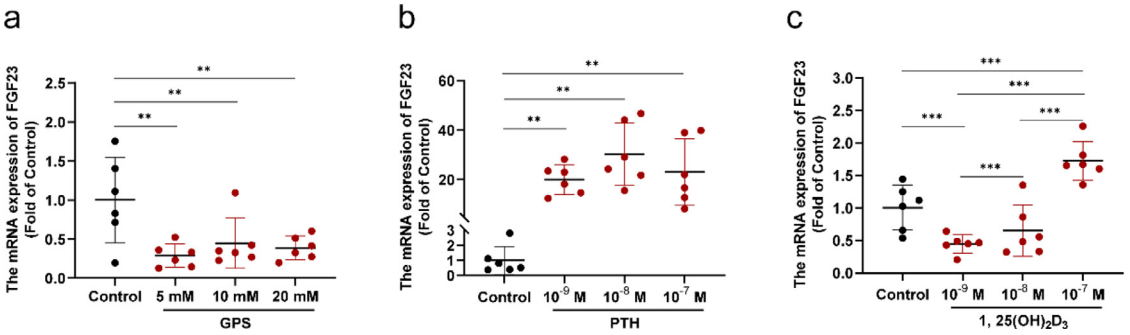

Figure 1. FGF23 is regulated by GPS, PTH and 1, 25(OH)$_2$D$_3$ in *in vitro*-cultured osteoblasts. The relative *FGF23* mRNA levels in osteoblasts treated with GPS (a), PTH (b) and 1, 25(OH)$_2$D$_3$ (c) for 48 h, respectively. Data are presented as Means ± SD (n = 6): $^{**}P < 0.05$, $^{***}P < 0.001$ vs. Control. GPS: β-glycerophosphate disodium salt; PTH: parathyroid hormone; 1, 25(OH)$_2$D$_3$: 1, 25-dihydroxyvitamin D3.

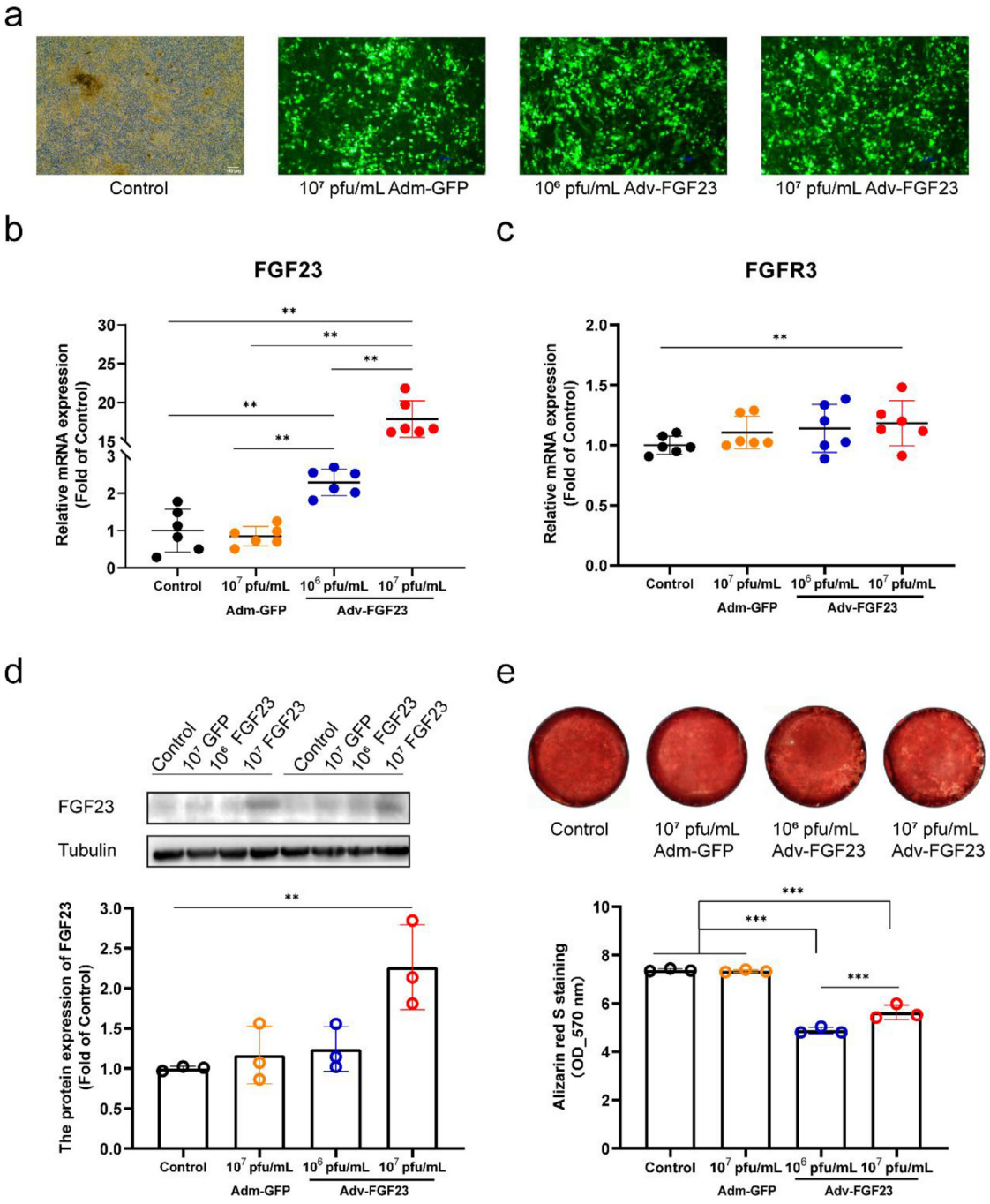

Figure 2. Overexpression of FGF23 inhibits osteoblast mineralization. The mineralized osteoblasts were treated with Adv-GFP (Vehicle) or Adv-FGF23 for 48 h. (a) The fluorescence observation of GFP in osteoblasts following infection of 10^7 pfu/mL Adv−GFP, 10^6 pfu/mL Adv−FGF23, and 10^7 pfu/mL Adv−FGF23, with no infection as a Control. Scale bar, 100 μm. (b-c) The mRNA expression of *FGF23* (b) and *FGFR3* (c) determined by real time qPCR (n = 6). β-actin was used as an internal control. (d) The protein expression of FGF23 (n = 3). Tubulin was used as an internal control. (e) Representative images and quantification of alizarin red S staining (n = 3). Data are presented as Means ± SD: $^{**}P < 0.05$, $^{***}P < 0.001$ vs. Control. Adv-GFP: empty vector adenovirus with GFP tagging; Adv-FGF23, FGF23 adenovirus; FGFR3, fibroblast growth factor receptor 3.

activity showed that Adv-FGF23 led to a significantly decreased in ALP activity ($P < 0.05$, Figure 3f). Contrary to the influence on *ALP* mRNA expression, the FGFR3 inhibitor was sufficient to increase the ALP activity both in the Adv-GFP group and Adv-FGF23 group ($P < 0.05$, Figure 3f), suggesting that the regulation of ALP by FGFR3 may be post-transcriptional. To explore possible mechanisms of FGF23 in osteoblast, the phosphorylated ERK (**P-ERK**) was assayed. The results showed that overexpression of Adv-FGF23 led to an increase in P-ERK versus the total ERK ratio ($P < 0.05$, Figure 3g). P-ERK failed to respond to 48h-FGFR3 inhibitor treatment ($P > 0.05$, Figure 3g). These data indicated that FGF23 is an inhibitor of BMSCs differentiation and mineralization. FGFR3 mediates the inhibition of FGF23 on ALP activity, but not for mineralization. The ERK signaling pathway is likely to be involved in the regulation of FGF23 on ALP activity.

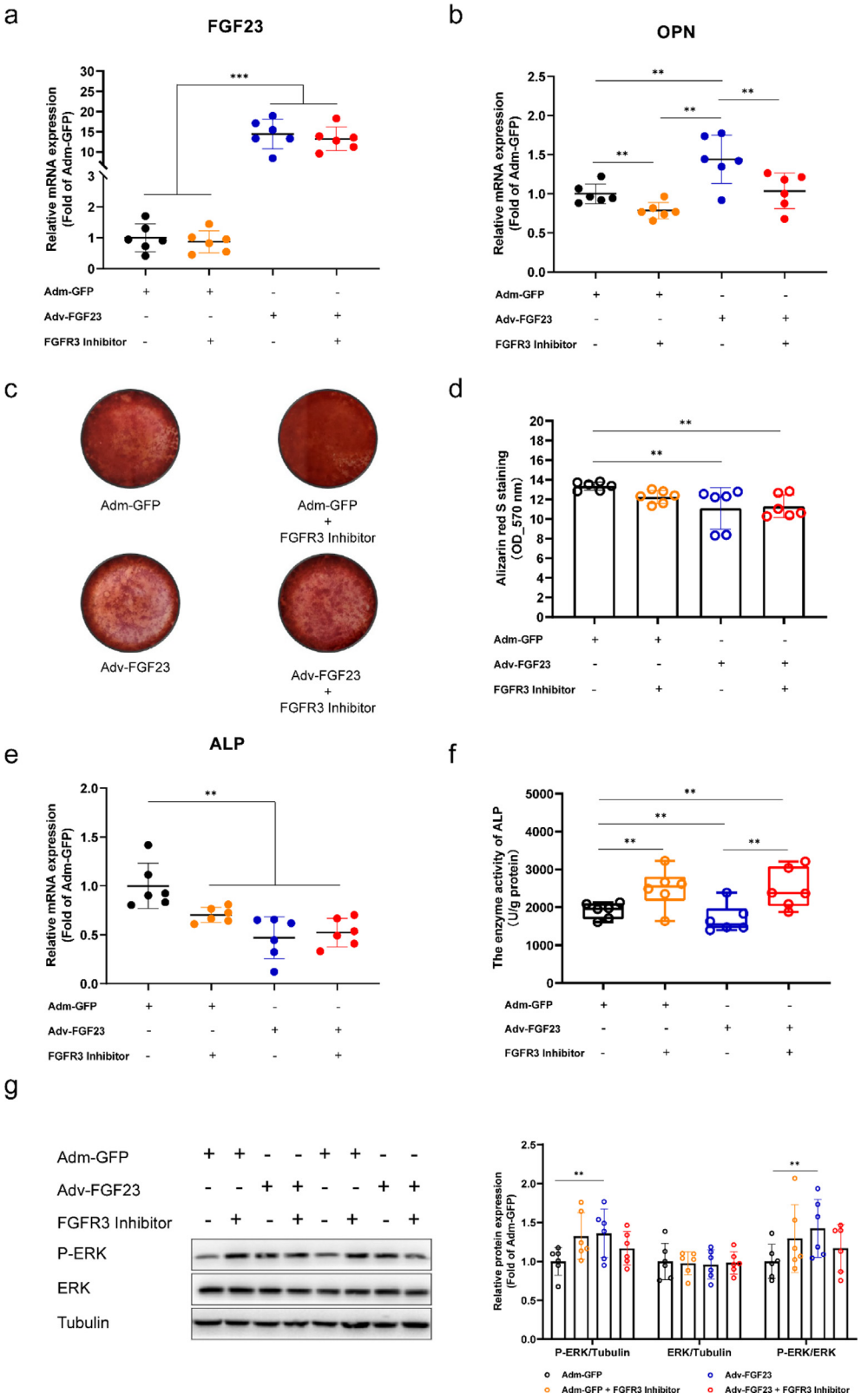

Figure 3. Blocking FGFR3 in mineralized osteoblasts restored the Adv-GF23 reduction of ALP activity without affecting extracellular mineralization. The mineralized osteoblasts were treated with Adv-FGF23 (10^7 pfu/mL) and/or FGFR3 inhibitor (50 nM) for 48 h. (a, b, e) Relative mRNA levels of *FGF23* (a), *OPN* (b), and *ALP* (e) determined by real-time qPCR (n = 6). β-actin was used as an internal control. (c-d) Representative images (c) and quantification of alizarin red S staining (d) (n = 3). (f) The enzyme activity of ALP, which is shown as U/g protein (n = 6). (g) Relative protein levels of P-ERK and ERK determined by Western blot (n = 6). Data are presented as Mean ± SD: $^{**}P < 0.05$, $^{***}P < 0.001$ vs. Adv-GFP. ALP, Alkaline phosphatase; FGFR3, fibroblast growth factor receptor 3; *OPN*: Osteopontin.

Effect of Co-Treatment with Adv-FGF23 and FGFR3 Inhibitor on Differentiated Osteoblasts

As mentioned above, FGFR3 inhibitor treatment for 48 h failed to restore the impaired cell mineralization caused by FGF23 overexpression. This might be due to the short treatment duration of the FGFR3 inhibitor. Thus, Adv-FGF23 was added at the beginning of BMSCs differentiation for 10 d to explore whether FGF23 regulates the osteogenic differentiation of BMSCs through FGFR3.

As shown in Figure 4a, infection of Adv-FGF23 upregulated *FGF23* mRNA expression by more than 1,000 times ($P < 0.001$). FGFR3 inhibitor caused a significant reduction of *FGF23* mRNA expression ($P < 0.001$, Figure 4a). While Adv-FGF23 increased the *OPN* mRNA level ($P < 0.05$, Figure 4b), the FGFR3 inhibitor could not only reduce the *OPN* mRNA expression alone but also blocked the Adv-FGF23 induction of OPN transcripts to the control level ($P < 0.05$, Figure 4b). Adv-FGF23 treatment for 10 d significantly inhibited the osteogenic mineralization of BMSCs, however, 10d-administration of FGFR3 inhibitor still failed to evoke any protective effects in restoring impaired mineralization of BMSCs ($P < 0.05$, Figure 4c, d). In agreement with the results in mineralized osteoblasts, *ALP* mRNA expression levels declined markedly following Adv-FGF23 treatment for 10 d ($P < 0.05$, Figure 4e). In Adv-GFP group, FGFR3 inhibitor down-regulated *ALP* mRNA expression ($P < 0.05$, Figure 4e). When co-treatment Adv-FGF23, FGFR3 inhibitor further reduced *ALP* mRNA expression, whose levels were comparable with the Adv-FGF23 group ($P < 0.05$, Figure 4e). Adv-FGF23 substantially reduced the ALP activity in differentiated osteoblasts ($P < 0.05$, Figure 4f). FGFR3 inhibitor was capable of preventing the Adv-FGF23-suppression of ALP activity ($P < 0.05$, Figure 4f). In addition, a significant upregulation of Adv-FGF23 was detected on P-ERK versus the total ERK ratio ($P < 0.05$, Figure 4g). FGFR3 inhibitor completely reversed the increased P-ERK protein content ($P < 0.05$, Figure 4g). These data demonstrated that FGF23 is an inhibitor of BMSCs ossification. FGFR3 is likely to mediate the regulation of FGF23 on ALP activity, but not BMSCs mineralization. The ERK signaling pathway was involved in the regulation of FGF23 on the osteogenic differentiation of BMSCs.

Effect of Co-Treatment with Adv-FGF23 and ERK Inhibitor on Mineralized Osteoblasts

To validate whether the ERK signaling pathway participates in the regulation of FGF23 on the ALP activity. An ERK-specific inhibitor (10 μM) was administrated in mineralized osteoblasts for 48 h. At the transcriptional level, ALP expression appeared to be unaffected by the ERK inhibitor ($P < 0.001$, Figure 5a). However, Adv-FGF23 led to a significant decrease in the ALP activity ($P < 0.001$, Figure 5b). The ERK inhibitor also tended to up-regulate the decreased ALP activity caused by FGF23 overexpression ($P = 0.08$, Figure 5b). The Adv-FGF23-induction of ERK phosphorylation was blocked by the ERK inhibitor ($P < 0.05$, Figure 5c). And the decreased ALP activity could be attributed to the rise of the P-ERK ($P < 0.05$, Figure 5b,c) because the ALP activity was significantly increased after blocking the ERK signaling pathway, even if it does not reach the level of Adv-GFP ($P < 0.05$, Figure 5c). These data indicated that FGF23 could regulate ALP activity through the ERK signaling pathway.

DISCUSSION

FGF23 Expression is Differently Influenced by P, 1, 25(OH)$_2$D$_3$, and PTH

FGF23 is considered to be one of the critical factors in inhibiting P reabsorption (Blau and Collins, 2015). Administration of recombinant FGF23 or its overexpression in animals induces hypophosphatemia and inhibition of Type IIa sodium-phosphate cotransporter (Shimada et al., 2001; Bai et al., 2003; Larsson et al., 2004). Besides, FGF23 suppresses the renal production of 1, 25(OH)$_2$D$_3$ by suppressing 1α-hydroxylase gene expression and stimulating *24-hydroxylase* mRNA expression (Shimada et al., 2004; Perwad et al., 2007). Klotho and FGFR1 are expressed not only in the kidney but also in other organs such as the parathyroid. FGF23 acts on the parathyroid to decrease serum PTH levels (Silver and Naveh-Many, 2012). On the contrary, P, 1, 25(OH)$_2$D$_3$, and PTH are also regulators of FGF23 expression.

We found that different concentrations of GPS inhibited the mRNA expression of *FGF23*, which is contrary to the results of studies on mammals. Weber et al. (2003) found that FGF23 was positively correlated with blood P levels in patients with X-linked hypophosphatemia (**Hyp**) (Weber et al., 2003). Perwad et al. (2005) have shown that the increase in P intake in the normal diet led to a dose-dependent increase in serum FGF23 concentration and skull *FGF23* mRNA expression (Perwad et al., 2005). We hypothesize that FGF23 excretes excess P intake through negative feedback. FGF23 does not play a P-excretion role in osteoblasts due to the inexistence of the P transport receptor. P is mainly involved in extracellular matrix mineralization, but the specific reasons for the down-regulation of FGF23 expression still need to be further explored.

The results we observed after PTH administration are consistent with the results of Kobayashi et al. (2006), that is, PTH significantly up-regulates the *FGF23* mRNA expression. It was found that the circulating FGF23 concentration in patients with primary hyperparathyroidism is very high, and is directly related to serum calcium and high concentration of PTH. After parathyroidectomy, the circulating FGF23 level is significantly reduced (Kobayashi et al., 2006). PTH

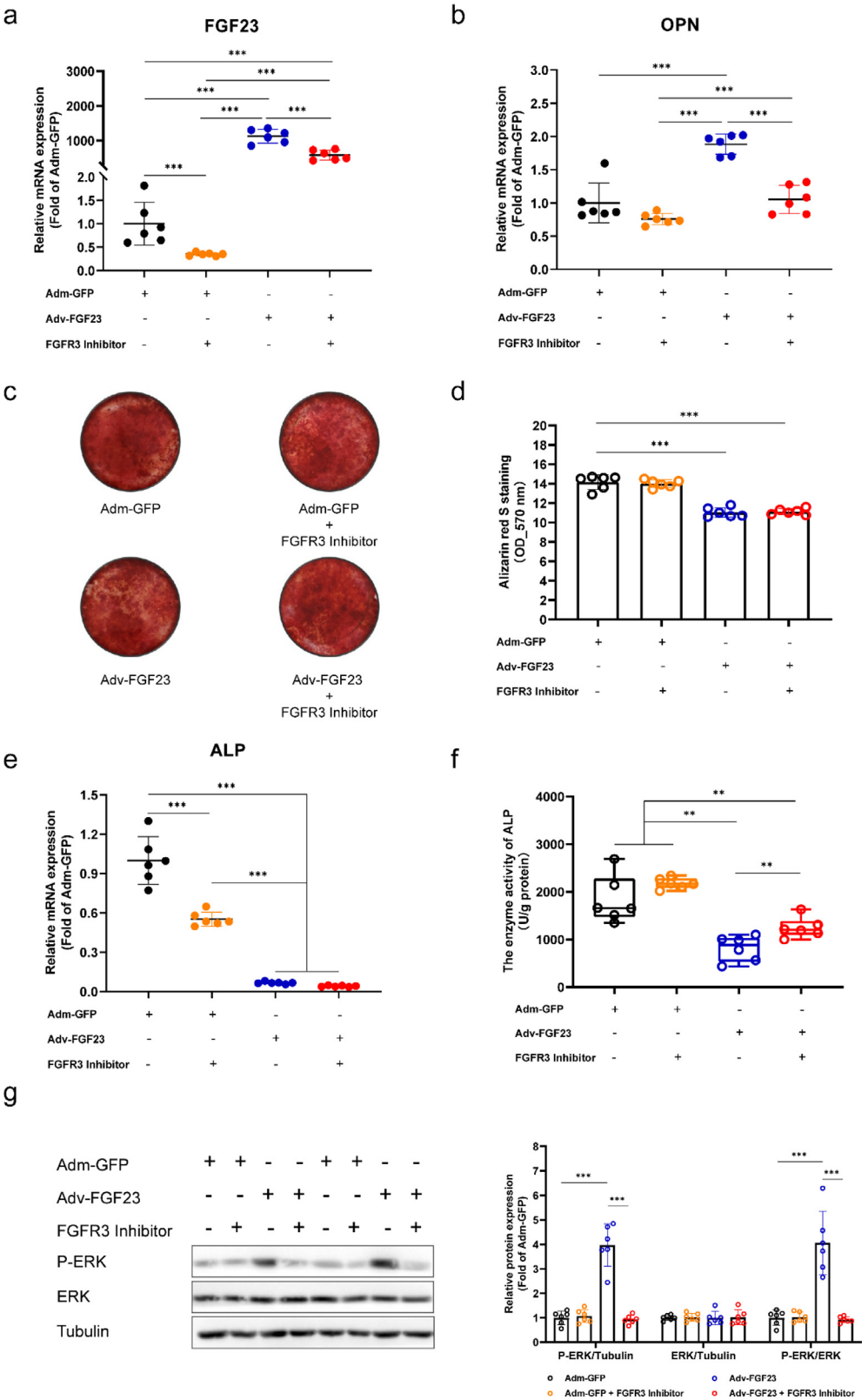

Figure 4. Blocking FGFR3 in differentiated osteoblasts rescued the reduced the Adv-FGF23-reduction of ALP activity and antagonized the Adv-FGF23-induction of ERK phosphorylation. The BMSCs were treated with Adv-FGF23 (10^7 pfu/mL) and/or FGFR3 inhibitor (50 nM) in the presence of osteogenic medium for 10 d. (a, b, e) Relative mRNA levels of *FGF23* (a), *OPN* (b), and *ALP* (e) determined by real-time qPCR (n = 6). β-actin was used as an internal control. (c-d) Representative images (c) and quantification of alizarin red staining (d) (n = 3). (f) The enzyme activity of ALP, which is shown as U/g protein (n = 6). (g) The protein expression and quantification of P-ERK and ERK, determined by Western blot (n = 6). Data are presented as Means ± SD: $^{**}P < 0.05$, $^{***}P < 0.001$ vs. Adv-GFP.

stimulates FGF23 production in osteoblasts by binding to the PTH1R and stimulating both the protein kinase A (**PKA**) and Wnt pathways (Lavi-Moshayoff et al., 2010). Regulation of FGF23 by PTH via the Wnt pathway is through inhibition of sclerostin, an inhibitor of the Wnt pathway (Wein et al., 2016; An et al., 2019).

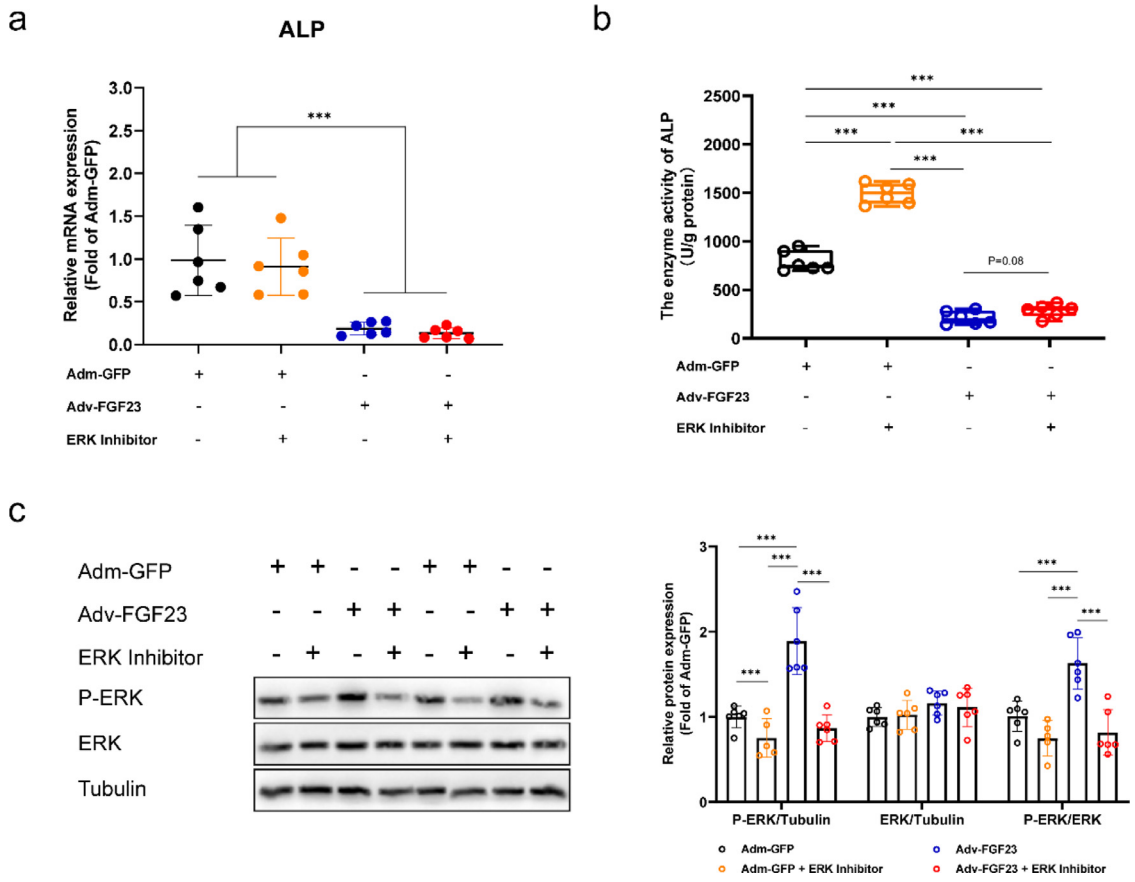

Figure 5. FGF23 regulates ALP activity through the ERK signaling pathway. Effect of Adv-FGF23 (10^7 pfu/mL) and ERK inhibitor (10 μM) on ALP mRNA expression (a), ALP activity, which is shown as U/g protein (b), and relative protein expression of P-ERK and ERK (c) for 48 h in BMSCs-differentiated osteoblasts. Data are presented as Means ± SD (n = 6): $^{***}P < 0.001$ vs. Adv-GFP.

Studies have shown that injection of 1, 25$(OH)_2D_3$ in normal mice increases serum FGF23 levels (Shimada et al., 2004). In normal and parathyroidectomy rats, the promotion of circulating FGF23 by 1, 25$(OH)_2D_3$ is in a dose-dependent manner (Saito et al., 2005). Also, the *FGF23* mRNA expression was up-regulated after 10^{-7} M 1, 25$(OH)_2D_3$ administration in UMR-106 (Kolek et al., 2005). However, we found that *FGF23* mRNA expression was not upregulated by all concentrations of 1, 25$(OH)_2D_3$. 10^{-9} M 1, 25$(OH)_2D_3$ had a significant inhibitory effect on *FGF23* mRNA expression, 10^{-8} M 1, 25$(OH)_2D_3$ did not affect *FGF23* mRNA expression, but 10^{-7} M 1, 25$(OH)_2D_3$ significantly up-regulated the *FGF23* mRNA expression. The reason for this difference may be related to the state of osteoblasts differentiation. Previous studies have also confirmed that different concentrations of 1, 25$(OH)_2D_3$ have opposite effects on osteoblast mineralization. It has been proved that 10^{-7} M 1, 25$(OH)_2D_3$ significantly reduced the calcium deposition in osteoblasts (Yamaguchi and Weitzmann, 2012). Research showed that under the condition of co-treatment with 10^{-9} M 1, 25$(OH)_2D_3$, and calcium chloride, the calcium deposition in osteoblasts increased significantly (Yang et al., 2015). FGF23 can be regulated by P, anemia, inflammation, PTH, 1, 25$(OH)_2D_3$, hypophosphatemia, insulin, and insulin-like growth factor 1 in osteoblasts and osteocytes in mammals (Agoro et al., 2020). Consistent with the previous reports, we found here that FGF23 expression is differently influenced by P, 1, 25$(OH)_2D_3$ and PTH in chicken osteoblasts.

FGF23 Suppresses Osteogenesis of BMSCs via the ERK Signaling

With the deepening of the research on FGF23, its function is multifaceted. In addition to regulating P and vitamin D metabolism, FGF23 directly regulates bone mineralization. The Hyp mice, whose serum levels of FGF23 are elevated, have low serum P and 1, 25$(OH)_2D_3$ levels, reduced expression of NPT2a in proximal tubules, and low bone mineral density (Liu et al., 2008). For FGF23-deficiency mice, their body weight, femur, tibia length, bone density, and trabecular bone volume were significantly reduced (Yuan et al., 2011). Shimada et al. (2004) indicated that FGF23 transgenic mice showed severe growth retardation after weaning with a round back, short skull, and increased unmineralized bone (Shimada et al., 2004). Research by Chen et al. (2011) showed that the mineral density of teeth and mandible of FGF23 transgenic mice was reduced, the expression of dentin saliva protein and the

deposition of type I collagen and osteocalcin in the dentin were significantly reduced (Chen et al., 2011).

To study the effect of FGF23 in bone remodeling, we overexpressed FGF23 in chicken osteoblasts via adenovirus. Osteoblasts successfully infected with Adv-FGF23 showed extremely strong GFP fluorescence. At the concentration of 10^7pfu/mL, the gene expression of FGF23 increased significantly. BMSCs with high expression of FGF23 were found to have lower ALP activity and weaker mineralization. Clinical study also demonstrated the negative relationships between serum FGF23 level and lumbar spine/proximal femur bone mineral density (BMD) in postmenopausal women (Shen et al., 2017), indicating that FGF23 is an inhibitor of osteogenic differentiation.

It has been established that different FGFRs mediate the role of FGF23 in different tissues. The regulation of FGF23 on P resorption in the kidney is Klotho-dependent (Ho and Bergwitz, 2021). But neither the serum phosphate nor 1, $25(OH)_2D_3$ levels were changed in FGFR3-null mice. Ablation of FGFR4 also failed to correct hypophosphatemia in Hyp mice (Liu et al., 2008). FGFR3 and FGFR4 do not mediate the renal effects of FGF23 (Liu et al., 2008). In addition, FGF23 regulates bone mineralization independently of Klotho, through interaction with FGFR3 in vitro (Murali et al., 2016). We found that FGF23 overexpression led to an increase in FGFR3 expression. We, therefore, examined whether FGF23 plays a regulatory role through FGFR3 in chicken osteoblasts by using an FGFR3 inhibitor.

In osteoblasts, only after the decomposition of pyrophosphate (**PPi**) into P under the action of TNAP, which is one of 4 ALP types, P is available for osteoblast mineralization (Orimo, 2010). PPi is an inhibitor of mineralization and is also a secretory stimulant of OPN (Beck et al., 2000; Beck and Knecht, 2003; Beck et al., 2003; Fatherazi et al., 2009). Overexpression of FGF23 significantly reduced the number of mineralized nodules, corresponding to the significantly up-regulated expression of *OPN* mRNA. FGFR3 inhibitor was found to block the upregulated levels of *OPN* mRNA expression induced by FGF23. Therefore, we hypothesized that FGF23 inhibited BMSCs differentiation into osteoblasts. Nonetheless, the inhibition of Adv-FGF23 on extracellular mineralization was not alleviated by the FGFR3 inhibitor. Furthermore, the ALP activity was determined, since ALP is a marker enzyme during osteoblasts differentiation and reflects the differentiation potential of osteoblasts (Long, 2011). Overexpression of FGF23 significantly inhibited ALP mRNA expression and activity, which is consistent with the results of Addison et al (Addison et al., 2007). Study also showed the inverse association of FGF23 with ALP in hemodialysis patients (Dörr et al., 2022). FGFR3 inhibitor also significantly inhibited ALP expression at the transcriptional level. Moreover, FGFR3 inhibitor can markedly restore the low ALP activity caused by Adv-FGF23, which indicated that FGF23 is likely to act post-transcriptionally through FGFR3 to regulate ALP activity. Previous studies have shown that FGF23 suppresses TNAP transcription and phosphate production in osteoblastic cells through FGFR3 independent of klotho, leading to a bone mineralization defect (Murali et al., 2016; Beck-Nielsen et al., 2019).

MAPK family members (ERK, JNK, p38) are involved in the formation of osteoblasts. Studies have shown that bone morphogenetic protein-mediated signal transduction transmits signals through MAPK, leading to the transcriptional activation of specific target genes involved in osteoblast differentiation and bone formation (Kakita et al., 2004; Lu et al., 2016). Low-dose tubulin promotes the proliferation and differentiation of BMSCs through the ERK pathway (Liang et al., 2019). Of note, the ERK signaling pathway is the upstream mediator of the Wnt signaling pathway, which is involved in promoting osteogenic differentiation of BMSCs and bone development (Krishnan et al., 2006; Baron and Kneissel, 2013; Carrillo-Lopez et al., 2016). Accordingly, overexpression of FGF23 resulted in significant up-regulation of P-ERK versus total ERK ratio in mineralized osteoblasts. Strikingly, the FGFR3 inhibitor was unable to alleviate the Adv-FGF23-induction of ERK phosphorylation.

We could interpret this from two aspects. On the one hand, the treatment time of 48 h with FGFR3 inhibitor was too short. On the other hand, the regulation of FGF23 on osteoblast extracellular matrix mineralization or phosphorylation of ERK was unrelated to FGFR3.

To further explore the mechanism underlying the role of FGF23, Adv-FGF23 was overexpressed during the first 10 d of BMSCs differentiation concurrent with treatment with an FGFR3 inhibitor. 10-day-treatment of FGFR3 inhibitor still failed to restore the decreased number of mineralized nodules induced by Adv-FGF23. The expression of OPN mRNA was not sufficient to reflect the degree of osteoblast mineralization. Consistent with the above results, the inhibition of ALP activity by FGF23 is mediated by FGFR3 in a post-transcriptional manner. Interestingly, 10-day-treatment of FGFR3 inhibitor not only blocked the inhibitory effect of FGF23 on ALP activity but also blocked P-ERK. Compared with the Adv-FGF23 group, P-ERK was significantly reduced after treatment with an FGFR3 inhibitor. These results suggest that ERK signaling pathway may be involved in the regulation of ALP activity by FGF23.

Next, we used an ERK inhibitor to examine whether the inhibition of FGF23 on ALP activity is related to ERK signaling. In mineralized osteoblasts, P-ERK was up-regulated and ALP activity decreases after overexpressing of FGF23. P-ERK was down-regulated with the administration of ERK inhibitor, resulting in a slight recovery of the ALP activity. These indicate that the inhibitory effect of FGF23 is, at least partially mediated through the FGF23-FGFR3-ERK pathway in chicken osteoblasts.

CONCLUSION

In summary, our data suggest that P, 1, 25$(OH)_2D_3$, PTH could affect FGF23 mRNA expression in chicken osteoblasts. FGF23 is an inhibitor of bone remodeling. FGF23 reduces ALP activity through the FGFR3-ERK signaling pathway in a post-transcriptional manner, thereby inhibiting the osteogenic ability of BMSCs. Additionally, FGF23 can also inhibit the mineralization of mature osteoblasts.

ACKNOWLEDGMENTS

This work was supported by the Key Technologies Research and Development Program of China (2021YFD1300405), the Earmarked Fund for China Agriculture Research System (CARS-40-K09), National Natural Science Foundation of China (31772619) and Key Technology Research and Development Program of Shandong Province (2019JZZY020602).

DISCLOSURES

The authors have declared no conflicts of interest.

REFERENCES

Addison, W. N., F. Azari, E. S. Sorensen, M. T. Kaartinen, and M. D. McKee. 2007. Pyrophosphate inhibits mineralization of osteoblast cultures by binding to mineral, up-regulating osteopontin, and inhibiting alkaline phosphatase activity. J. Biol. Chem. 282:15872–15883.

Agoro, R., P. Ni, M. L. Noonan, and K. E. White. 2020. Osteocytic FGF23 and its kidney function. Front. Endocrinol. (Lausanne) 11:592.

Ahmad, H., and R. J. J. o. A. P. R. Balander. 2003. Alternative feeding regimen of calcium source and phosphorus level for better eggshell quality in commercial layers. 12:509-514.

Alizadeh Naderi, A. S., and R. F. Reilly. 2010. Hereditary disorders of renal phosphate wasting. Nat. Rev. Nephrol. 6:657–665.

An, Y., J. Zhao, F. Nie, Y. Wu, Y. Xia, and D. Li. 2019. Parathyroid hormone (PTH) promotes ADSC osteogenesis by regulating SIK2 and Wnt4. Biochem. Biophys. Res. Commun 516:551–557.

Bai, X. Y., D. Miao, D. Goltzman, and A. C. Karaplis. 2003. The autosomal dominant hypophosphatemic rickets R176Q mutation in fibroblast growth factor 23 resists proteolytic cleavage and enhances in vivo biological potency. J. Biol. Chem. 278:9843–9849.

Baron, R., and M. Kneissel. 2013. WNT signaling in bone homeostasis and disease: from human mutations to treatments. Natl. Med. 19:179–192.

Beck-Nielsen, S. S., Z. Mughal, D. Haffner, O. Nilsson, E. Levtchenko, G. Ariceta, C. de Lucas Collantes, D. Schnabel, R. Jandhyala, and O. Mäkitie. 2019. FGF23 and its role in X-linked hypophosphatemia-related morbidity. Orphanet. J. Rare Dis. 14:58.

Beck, G. R. Jr., and N. Knecht. 2003. Osteopontin regulation by inorganic phosphate is ERK1/2-, protein kinase C-, and proteasome-dependent. J. Biol. Chem. 278:41921–41929.

Beck, G. R. Jr., E. Moran, and N. Knecht. 2003. Inorganic phosphate regulates multiple genes during osteoblast differentiation, including Nrf2. Exp. Cell Res. 288:288–300.

Beck, G. R. Jr., B. Zerler, and E. Moran. 2000. Phosphate is a specific signal for induction of osteopontin gene expression. Proc. Natl. Acad. Sci. USA 97:8352–8357.

Blau, J. E., and M. T. Collins. 2015. The PTH-Vitamin D-FGF23 axis. Rev. Endocrine Metab. Disorders 16:165–174.

Carrillo-Lopez, N., S. Panizo, C. Alonso-Montes, P. Roman-Garcia, I. Rodriguez, C. Martinez-Salgado, A. S. Dusso, M. Naves, and J. B. Cannata-Andia. 2016. Direct inhibition of osteoblastic Wnt pathway by fibroblast growth factor 23 contributes to bone loss in chronic kidney disease. Kidney Int. 90:77–89.

Chen, L., H. Liu, W. Sun, X. Bai, A. C. Karaplis, D. Goltzman, and D. Miao. 2011. Fibroblast growth factor 23 overexpression impacts negatively on dentin mineralization and dentinogenesis in mice. Clin. Exp. Pharmacol. Physiol. 38:395–402.

Consortium, A. 2000. Autosomal dominant hypophosphataemic rickets is associated with mutations in FGF23. Nat. Genetics 26:345–348.

Dörr, K., S. Hödlmoser, M. Kammer, R. Reindl-Schwaighofer, M. Lorenz, B. Reiskopf, R. Jagoditsch, R. Marculescu, and R. Oberbauer. 2022. Bone specific alkaline phosphatase and serum calcification propensity are not influenced by etelcalcetide vs. alfacalcidol treatment, and only bone specific alkaline phosphatase is correlated with fibroblast growth factor 23: Sub-analysis results of the ETACAR-HD study. Front. Med. (Lausanne) 9:948177.

Eleuteri, S., and A. Fierabracci. 2019. Insights into the secretome of mesenchymal stem cells and its potential applications. Int. J. Mol. Sci. 20:4597.

Erben, R. G. 2018. Physiological actions of fibroblast growth factor-23. Front. Endocrinol. (Lausanne) 9:267.

Fatherazi, S., D. Matsa-Dunn, B. L. Foster, R. B. Rutherford, M. J. Somerman, and R. B. Presland. 2009. Phosphate regulates osteopontin gene transcription. J. Dental Res. 88:39–44.

Fernandes-Freitas, I., and B. M. Owen. 2015. Metabolic roles of endocrine fibroblast growth factors. Curr. Opin. Pharmacol. 25:30–35.

Fierabracci, A., A. Del Fattore, R. Luciano, M. Muraca, A. Teti, and M. Muraca. 2015. Recent advances in mesenchymal stem cell immunomodulation: the role of microvesicles. Cell Transpl. 24:133–149.

Fleming, R. H., H. A. McCormack, L. McTeir, and C. C. Whitehead. 1998. Medullary bone and humeral breaking strength in laying hens. Res. Vet. Sci. 64:63–67.

Hadley, J. A., M. Horvat-Gordon, W. K. Kim, C. A. Praul, D. Burns, and R. M. Leach Jr. 2016. Bone sialoprotein keratan sulfate proteoglycan (BSP-KSPG) and FGF-23 are important physiological components of medullary bone. Compar. Biochem. Physiol. Part A Mol. Integr. Physiol. 194:1–7.

Ho, B. B., and C. Bergwitz. 2021. FGF23 signalling and physiology. J. Mol. Endocrinol. 66:R23–r32.

Kakita, A., A. Suzuki, Y. Ono, Y. Miura, M. Itoh, and Y. Oiso. 2004. Possible involvement of p38 MAP kinase in prostaglandin E1-induced ALP activity in osteoblast-like cells. Prostaglandins Leukotrienes Essential Fatty Acids 70:469–474.

Kerschnitzki, M., T. Zander, P. Zaslansky, P. Fratzl, R. Shahar, and W. Wagermaier. 2014. Rapid alterations of avian medullary bone material during the daily egg-laying cycle. Bone 69:109–117.

Kobayashi, K., Y. Imanishi, A. Miyauchi, N. Onoda, T. Kawata, H. Tahara, H. Goto, T. Miki, E. Ishimura, T. Sugimoto, T. Ishikawa, M. Inaba, and Y. Nishizawa. 2006. Regulation of plasma fibroblast growth factor 23 by calcium in primary hyperparathyroidism. Eur. J. Endocrinol. 154:93–99.

Kolek, O. I., E. R. Hines, M. D. Jones, L. K. LeSueur, M. A. Lipko, P. R. Kiela, J. F. Collins, M. R. Haussler, and F. K. Ghishan. 2005. 1alpha,25-Dihydroxyvitamin D3 upregulates FGF23 gene expression in bone: the final link in a renal-gastrointestinal-skeletal axis that controls phosphate transport. Am. J. Physiol. Gastroint. Liver Physiol. 289:G1036–G1042.

Krishnan, V., H. U. Bryant, and O. A. Macdougald. 2006. Regulation of bone mass by Wnt signaling. J. Clin. Investig. 116:1202–1209.

Kurosu, H., Y. Ogawa, M. Miyoshi, M. Yamamoto, A. Nandi, K. P. Rosenblatt, M. G. Baum, S. Schiavi, M. C. Hu, O. W. Moe, and M. Kuro-o. 2006. Regulation of fibroblast growth factor-23 signaling by klotho. J. Biol. Chem. 281:6120–6123.

Larsson, T., R. Marsell, E. Schipani, C. Ohlsson, O. Ljunggren, H. S. Tenenhouse, H. Jüppner, and K. B. Jonsson. 2004. Transgenic mice expressing fibroblast growth factor 23 under the control of the alpha1(I) collagen promoter exhibit growth retardation, osteomalacia, and disturbed phosphate homeostasis. Endocrinology 145:3087–3094.

Lavi-Moshayoff, V., G. Wasserman, T. Meir, J. Silver, and T. Naveh-Many. 2010. PTH increases FGF23 gene expression and mediates the high-FGF23 levels of experimental kidney failure: a

bone parathyroid feedback loop. Am. J. Physiol. Renal Physiol. 299:F882–F889.
Li, P., R. Wang, H. Jiao, X. Wang, J. Zhao, and H. Lin. 2018. Effects of dietary phosphorus level on the expression of calcium and phosphorus transporters in laying hens. Front. Physiol. 9:627.
Li, Y., X. He, H. Olauson, T. E. Larsson, and U. Lindgren. 2013. FGF23 affects the lineage fate determination of mesenchymal stem cells. Calcified Tissue Int. 93:556–564.
Liang, J. Q., F. Lu, B. Gan, Y. Y. Wen, J. Chen, H. G. Wang, Y. Yang, X. S. Peng, and Y. F. Zhou. 2019. Low-dose tubacin promotes BMSCs proliferation and morphological changes through the ERK pathway. Am. J. Transl. Res. 11:1446–1459.
Liu, S., L. Vierthaler, W. Tang, J. Zhou, and L. D. Quarles. 2008. FGFR3 and FGFR4 do not mediate renal effects of FGF23. J. Am. Soc. Nephrol. 19:2342–2350.
Long, F. 2011. Building strong bones: molecular regulation of the osteoblast lineage. Nat. Rev. Mol. Cell Biol. 13:27–38.
Lu, D. G., J. N. Qu, J. L. Lei, P. F. Wang, C. Sun, L. K. Huang, D. Tian, Z. Song, W. Wei, Z. Li, and K. Zhang. 2016. LPS-stimulated inflammation inhibits BMP-9-induced osteoblastic differentiation through crosstalk between BMP/MAPK and Smad signaling. Exp. Cell Res. 341:54–60.
Murali, S. K., P. Roschger, U. Zeitz, K. Klaushofer, O. Andrukhova, and R. G. Erben. 2016. FGF23 regulates bone mineralization in a 1,25(OH)2 D3 and Klotho-independent manner. J. Bone Mineral Res. 31:129–142.
Niu, H., H. Song, Y. Guan, X. Zong, R. Niu, S. Zhao, C. Liu, W. Yan, W. Guan, and X. Wang. 2021. Chicken bone marrow mesenchymal stem cells improve lung and distal organ injury. Sci. Rep. 11:17937.
Okamoto, K., T. Nakashima, M. Shinohara, T. Negishi-Koga, N. Komatsu, A. Terashima, S. Sawa, T. Nitta, and H. Takayanagi. 2017. Osteoimmunology: the conceptual framework unifying the immune and skeletal systems. Physiol. Rev. 97:1295–1349.
Orimo, H. 2010. The mechanism of mineralization and the role of alkaline phosphatase in health and disease. J. Nippon Med. School 77:4–12.
Pande, V. V., K. C. Chousalkar, M. S. Bhanugopan, and J. C. Quinn. 2015. Super pharmacological levels of calcitriol (1,25-(OH)2D3) inhibits mineral deposition and decreases cell proliferation in a strain dependent manner in chicken mesenchymal stem cells undergoing osteogenic differentiation in vitro. Poultry Sci. 94:2784–2796.
Perwad, F., N. Azam, M. Y. Zhang, T. Yamashita, H. S. Tenenhouse, and A. A. Portale. 2005. Dietary and serum phosphorus regulate fibroblast growth factor 23 expression and 1,25-dihydroxyvitamin D metabolism in mice. Endocrinology 146:5358–5364.
Perwad, F., M. Y. Zhang, H. S. Tenenhouse, and A. A. Portale. 2007. Fibroblast growth factor 23 impairs phosphorus and vitamin D metabolism in vivo and suppresses 25-hydroxyvitamin D-1alpha-hydroxylase expression in vitro. Am. J. Physiol. Renal Physiol. 293:F1577–F1583.
Ren, Z., M. Ebrahimi, D. E. Butz, J. M. Sand, K. Zhang, and M. E. Cook. 2017. Antibody to fibroblast growth factor 23-peptide reduces excreta phosphorus of laying hens. Poultry Sci. 96:127–134.
Saito, H., A. Maeda, S. Ohtomo, M. Hirata, K. Kusano, S. Kato, E. Ogata, H. Segawa, K. Miyamoto, and N. Fukushima. 2005. Circulating FGF-23 is regulated by 1alpha,25-dihydroxyvitamin D3 and phosphorus in vivo. J. Biol. Chem. 280:2543–2549.
Schreiweis, M. A., J. I. Orban, M. C. Ledur, and P. Y. Hester. 2003. The use of densitometry to detect differences in bone mineral density and content of live White Leghorns fed varying levels of dietary calcium. Poultry Sci. 82:1292–1301.
Shen, J., S. Fu, and Y. Song. 2017. Relationship of fibroblast growth factor 23 (FGF-23) serum levels with low bone mass in postmenopausal women. J. Cell. Biochem. 118:4454–4459.
Shimada, T., H. Hasegawa, Y. Yamazaki, T. Muto, R. Hino, Y. Takeuchi, T. Fujita, K. Nakahara, S. Fukumoto, and T. Yamashita. 2004. FGF-23 is a potent regulator of vitamin D metabolism and phosphate homeostasis. J. Bone Mineral Res. 19:429–435.
Shimada, T., S. Mizutani, T. Muto, T. Yoneya, R. Hino, S. Takeda, Y. Takeuchi, T. Fujita, S. Fukumoto, and T. Yamashita. 2001. Cloning and characterization of FGF23 as a causative factor of tumor-induced osteomalacia. In Proc. Natl. Acad. Sci. USA: (pp. 6500−6505) *98*6500–6505.
Shimada, T., I. Urakawa, Y. Yamazaki, H. Hasegawa, R. Hino, T. Yoneya, Y. Takeuchi, T. Fujita, S. Fukumoto, and T. Yamashita. 2004. FGF-23 transgenic mice demonstrate hypophosphatemic rickets with reduced expression of sodium phosphate cotransporter type IIa. Biochem. Biophys. Res. Commun. 314:409–414.
Silver, J., and T. Naveh-Many. 2012. FGF23 and the parathyroid. Adv. Exp. Med. Biol. 728:92–99.
Simic, P., and J. L. Babitt. 2021. Regulation of FGF23: beyond bone. Curr. Osteoporosis Rep. 19:563–573.
Svoradova, A., V. Zmrhal, E. Venusova, and P. Slama. 2021. Chicken mesenchymal stem cells and their applications: a mini review. Animals (Basel) 11.
Tan, J., X. Xu, Z. Tong, J. Lin, Q. Yu, Y. Lin, and W. Kuang. 2015. Decreased osteogenesis of adult mesenchymal stem cells by reactive oxygen species under cyclic stretch: a possible mechanism of age related osteoporosis. Bone Res. 3:15003.
Urakawa, I., Y. Yamazaki, T. Shimada, K. Iijima, H. Hasegawa, K. Okawa, T. Fujita, S. Fukumoto, and T. Yamashita. 2006. Klotho converts canonical FGF receptor into a specific receptor for FGF23. Nature 444:770–774.
Wang, R. M., J. P. Zhao, X. J. Wang, H. C. Jiao, J. M. Wu, and H. Lin. 2018. Fibroblast growth factor 23 mRNA expression profile in chickens and its response to dietary phosphorus. Poultry Sci. 97:2258–2266.
Weber, T. J., S. Liu, O. S. Indridason, and L. D. Quarles. 2003. Serum FGF23 levels in normal and disordered phosphorus homeostasis. J. Bone Mineral Res. 18:1227–1234.
Wein, M. N., Y. Liang, O. Goransson, T. B. Sundberg, J. Wang, E. A. Williams, M. J. O'Meara, N. Govea, B. Beqo, S. Nishimori, K. Nagano, D. J. Brooks, J. S. Martins, B. Corbin, A. Anselmo, R. Sadreyev, J. Y. Wu, K. Sakamoto, M. Foretz, R. J. Xavier, R. Baron, M. L. Bouxsein, T. J. Gardella, P. Divieti-Pajevic, N. S. Gray, and H. M. Kronenberg. 2016. SIKs control osteocyte responses to parathyroid hormone. Nat. Commun. 7:13176.
Whitehead, C. C. 2004. Overview of bone biology in the egg-laying hen. Poultry Sci. 83:193–199.
Yamaguchi, M., and M. N. Weitzmann. 2012. High dose 1,25(OH) 2D3 inhibits osteoblast mineralization in vitro. Int. J. Mol. Med. 29:934–938.
Yang, D., A. G. Turner, A. R. Wijenayaka, P. H. Anderson, H. A. Morris, and G. J. Atkins. 2015. 1,25-Dihydroxyvitamin D3 and extracellular calcium promote mineral deposition via NPP1 activity in a mature osteoblast cell line MLO-A5. Mol. Cellular Endocrinol. 412:140–147.
Yoshiko, Y., H. Wang, T. Minamizaki, C. Ijuin, R. Yamamoto, S. Suemune, K. Kozai, K. Tanne, J. E. Aubin, and N. Maeda. 2007. Mineralized tissue cells are a principal source of FGF23. Bone 40:1565–1573.
Yuan, Q., T. Sato, M. Densmore, H. Saito, C. Schuler, R. G. Erben, and B. Lanske. 2011. FGF-23/Klotho signaling is not essential for the phosphaturic and anabolic functions of PTH. J. Bone Mineral Res. 26:2026–2035.